Russian Chemical Reviews **70** (7) 535 – 541 (2001) © 2001 Russian Academy of Sciences and Turpion Ltd

DOI 10.1070/RC2001v070n07ABEH000652

Paramagnetic resonance and detection of a single electron spin

A L Buchachenko, F I Dalidchik, S A Kovalevskii, B R Shub

Contents

I.	Introduction	535
II.	ESR sensitivity evolution	535
III.	Optical detection and magnetic resonance of single triplet molecules	536
IV.	Single-molecule tunnelling spectroscopy	537
V.	Tunnelling spectroscopy of a single electron spin	538
VI.	Tunneling spectroscopy of spin channels	538
VII.	Single electron spin relaxation	539
VIII.	Can single-spin ESR be detected by tunnelling spectroscopy?	539
IX.	Excited states and single-molecule chemistry	540
X.	Single-molecule spin chemistry	541
XI.	Conclusion	541

Abstract. Two methods of detection of a single electron spin, namely, optical detection (1993) and tunnelling spectroscopy (1998) are described. Both methods are based on the spin chemistry laws. Physical principles and prospects of application of these methods are considered. The bibliography includes 34 references.

I. Introduction

Electron spin resonance (ESR) spectroscopy has found numerous applications in physics, chemistry, molecular biology and medicine. This method has two key functions. First, it is used as a physical tool in studies of the structure and dynamics of spin carriers (radicals, ions, complexes, high-spin molecules, *etc*.). The hyperfine (electron – nucleus) interaction constants as well as the magnitudes of dipole (electron – electron) splitting of the Zeeman energy levels and the parameters of spin – orbit interaction, which manifests itself as different values of *g*-factors, contain structural information. The width and shape of ESR spectral lines contain information on the rotational, translational and intramolecular spin carrier dynamics. This information can be extracted by means of the spin relaxation times τ_1 and τ_2 which are determined by the rate of energy relaxation of the Zeeman reservoir and the rate of phase relaxation (*i.e*., spin precession) respectively.

Second, ESR spectroscopy is an important analytical method which is used not only in fundamental areas of science (physics, chemistry and biology), but also in ecology, archaeology, medicine and history (*e.g*., in age determination using ESR[1,2]). Analytically, the key advantage of this method is its high sensitivity. The aim of this review is to analyse the evolution of this parameter and to outline some ways toward progress in reaching the limiting sensitivity, which allows detection of a single, individual paramagnetic species.

A L Buchachenko, F I Dalidchik, S A Kovalevskii, B R Shub N N Semenov Institute of Chemical Physics, Russian Academy of Sciences, ul. Kosygina 4, 119991 Moscow, Russian Federation. Fax (7-095) 938 24 84.
Tel. (7-095) 939 74 90. E-mail: spinchem@chph.ras.ru
(A L Buchachenko)
Tel. (7-095) 939 72 59 (F I Dalidchik), (7-095) 137 82 73 (B R Shub)

Received 15 January 2001
Uspekhi Khimii **70** (7) 611 – 618 (2001); translated by A M Raevsky

II. ESR sensitivity evolution

In his pioneering paper Zavoiskii reported a sensitivity of $\sim 10^{19}$ spins. In 1959, Semenov and Bubnov[3] improved the ESR sensitivity and reached a value of $\sim 10^{11}$ spins using high-frequency modulation and automatic frequency control. Since then this value appeared to be a 'nearly limiting' one for all commercial ESR spectrometers including modern instruments. Further improvement of sensitivity up to $\sim 10^7$ spins[4] appeared to be solely due to the development of high-resolution ESR spectroscopy (an 'elite' division of ESR spectroscopy) which operates with magnetic fields of ~ 50 kŒ. The sensitivity of 'routine' ESR spectroscopy is, as a rule, $\sim 10^{11}$.

Technically, this threshold is difficult to overcome since it is determined by the low sensitivity of detectors of microwave and radiofrequency radiation (it should be remembered that classical ESR spectroscopy is based on measurements of energy losses).

A great breakthrough in studies aimed at improving the ESR sensitivity is associated with the use of a combination of the microwave pumping of the spin system with optical detection of results. High photon energy allows them to be detected even in the photon-counting regime. This provides a colossal gain in sensitivity and starts the development of non-classical ESR spectroscopy, *viz*., the so-called optically detected magnetic resonance (ODMR).

The principle of ODMR is illustrated in Fig. 1. Let us assume that a triplet radical pair with the total spin $S = 1$ is generated by photolysis or radiolysis in solution or in a solid. In the magnetic field, only two spin states are mixed. These are the triplet state T_0 with the zero spin projection and the singlet state S, whereas the other two spin states (T_+ and T_-) with the spin projections $S_z = \pm 1$ are excluded from the triplet – singlet intersystem crossing of the pair. Fast intersystem crossing from the non-reactive state T_0 to the reactive state S followed by the formation of reaction products in the radical pair leads to depopulation of the levels T_0 and S. Microwave pumping at the ESR frequency ω corresponding to the difference between the Zeeman energies of

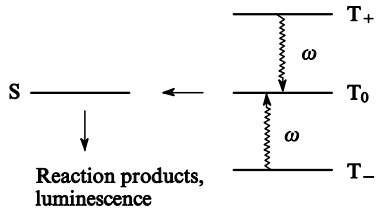


Figure 1. An energy level diagram illustrating the ODMR mechanism. Here and in Fig. 2 wavy arrows denote the microwave pumping of corresponding transitions.

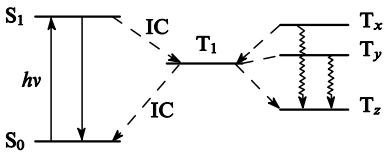


Figure 2. An energy level diagram illustrating transitions between different levels in the pentacene molecule.
Notations of energy levels: S_0 and S_1 are the ground-state singlet and excited singlet levels, respectively; T_1 is the lowest triplet state; T_x, T_y and T_z are the magnetic sublevels of the triplet state T_1. IC denotes intersystem crossing.

the states T_0-T_+ and T_0-T_- leads to an inversion drop and accumulation of electron spins on the level T_0, thus increasing the yield of reaction products. Clearly, the radical pair serves as a chemical microwave detector. If reaction products fluoresce, 'chemical reception' of microwaves can be optically detected, which is the case with ODMR. However, this is not the only reception technique since in the case of charged reaction products magnetic resonance can be detected using changes in conductivity. Generally, this technique is well known as Reaction Yield Detected Magnetic Resonance (RYDMR). Pioneering studies on RYDMR were reported by Frankevich.[5,6] Among different versions of the RYDMR method, ODMR is the most sensitive one.

The outstanding possibilities of the ODMR technique can be best illustrated by the results obtained by Molin *et al.*[7,8] taking detection of aromatic radical anions as an example. Generation of anion–cation radical pairs in the experiments on radiolysis of solutions of aromatic molecules is followed by their annihilation and creation of electronically excited luminescent molecules. The yield of such molecules is strongly dependent on the microwave pumping of ESR transitions in the radical pair. In this case the ODMR sensitivity is as high as several tens of spins. It should be noted that both pulsed and CW ODMR can be observed experimentally.

Having reached such a high sensitivity, it is logical to pose the next problem which can be formulated as detection of single-molecule ESR (or ESR of a single electron spin carrier).

III. Optical detection and magnetic resonance of single triplet molecules

Progress in photodetection technique and confocal optical microscopy has opened the possibility of visual observation and optical detection of single molecules.[9] Upon being illuminated, luminescent molecules (*e.g.*, rhodamine 6G, terrylenediimine, *etc.*) adsorbed on a surface, implanted (in low concentrations) in monomolecular layers or embedded in thin polymer films can be observed as molecular 'fireflies' using a microscope. Currently, this experimental technique has been intensely developed. It is widely used in, *e.g.*, molecular dynamics studies. Translational dynamics are studied by tracing the 'firefly' trajectory while information on rotational dynamics is obtained by measuring luminescence depolarisation. Other areas of application of the 'firefly' technique include measurements of the rates of energy transfer to neighbouring molecules, verification of the ergodic theorem, *etc.*[10,11]

Many optical chromophores used in the experiments on observation of single molecules occur in the long-lived triplet states. By placing such molecules in a permanent and a microwave magnetic field one can initiate paramagnetic resonance and detect it optically by means of observation of light emission from the molecular 'fireflies'. The possibility of using such a detection technique can be aptly illustrated taking the ODMR of single pentacene molecules in a *p*-terphenyl single crystal (the mole fraction of pentacene was $\sim 10^{-8}$) as an example. *A propos*, it is this system that was used in the first successful single-molecule ODMR experiments.[12,13]

An energy level diagram of pentacene spins, typical of almost all molecules, is shown in Fig. 2. After absorption of a quantum $h\nu$, the molecule goes from the ground state S_0 to the excited state S_1 which is then depopulated *via* fluorescence or molecular relaxation to the lowest triplet state T_1. The state T_1 is paramagnetic and triply spin degenerate. The dipole interaction between two spins leads to removal of degeneracy and the appearance of three energy levels (T_x, T_y and T_z).

The dipole electron–electron interaction is described by a tensor, the principal components of which, ε_x, ε_y and ε_z, are different with respect to different molecular axes. In ESR spectroscopy, they are usually expressed through the parameters D and E.

$$D = \frac{3}{2}\varepsilon_z,\ E = -\frac{1}{2}(\varepsilon_x - \varepsilon_y).$$

These parameters characterise the deviation of the symmetry of the dipole interaction (and, hence, spin distribution) from spherical and axial symmetry, respectively.

Dipole splitting also exists in the absence of a magnetic field. If a molecule is placed in an external magnetic field, one should take into account not only the dipole magnetic interaction, but also the Zeeman magnetic interaction, so that in the limiting case (in strong magnetic fields) the spin states T_x, T_y and T_z with the energies ε_x, ε_y and ε_z, respectively, are transformed into the corresponding canonical spin states T_+, T_0 and T_-.

Intersystem crossing from the state S_1 to the state T_1 is spin-forbidden and is thus induced by the intramolecular spin–orbit interaction, which partially removes this forbiddenness (due to exchange between the intrinsic angular momentum of an electron and its orbital angular momentum). Since the orbital angular momentum is anisotropic (*i.e.*, it takes different values with respect to different molecular axes), the spin–orbit interaction is also anisotropic. Because of this, the rate of inversion drop from the state S_1 also appears to be dependent on the symmetry of the molecule: the states T_x, T_y and T_z with the energies ε_x, ε_y and ε_z (and, correspondingly, the states T_+, T_0 and T_-) are populated at different rates.

For the same reason, the depopulation rates of these levels due to spin relaxation from the state T_1 to the ground state are also different. These differences in the population and depopulation rates of the three spin sublevels of the triplet T_1 are responsible for colossal differences in their steady-state populations. For instance, excitation of a pentacene molecule to the state S_1 followed by red $S_1 \rightarrow S_0$ fluorescence also causes population of the lowest triplet level T_1 with a probability of 0.5%. Among the triplet sublevels, the highest population rates ($1.5 \times 10^5\ s^{-1}$) are observed for the levels T_x and T_y; the depopulation rates of these levels (transition to the ground state S_0) are also high ($0.25 \times 10^5\ s^{-1}$).

For the level T_z, these rates are very low, so that in the steady-state regime only the levels T_x and T_y appear to be populated, whereas the level T_z remains nearly completely depopulated.

If microwave pumping is tuned to resonance with the energy difference between the spin levels T_x and T_z, their populations are

equalised. As a result, a proportion of pentacene molecules pass to the long-lived T_z level and are temporarily excluded from the 'community' of fluorescent molecules.

Clearly, a decrease in the fluorescence intensity of a single pentacene molecule is an indicator of magnetic resonance. Knowing the kinetic constants of photophysical and relaxation processes, one can estimate the magnitude of this effect: it reaches $\sim 20\%$ in the case of microwave pumping of the transition $T_x - T_z$.[13]

An ODMR spectrum of a single triplet pentacene molecule is shown in Fig. 3 *a*. In accord with theory, microwave pumping at the resonance frequencies of the $T_x - T_z$ and $T_y - T_z$ transitions (~ 1470 and ~ 1410 MHz, respectively) leads to noticeable (by more than 10%) decrease in the fluorescence intensity; the latter transition is less intense since the population of the level T_y is intermediate between those of the 'active' (T_x) and 'passive' (T_z) levels.

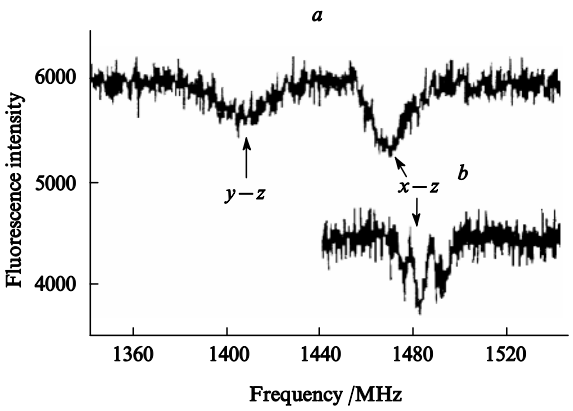


Figure 3. An ODMR spectrum of a single pentacene molecule implanted in a *p*-terphenyl crystal (*a*) and hyperfine structure of the ODMR spectrum of a pentacene molecule deuterated at all positions except for two positions at the carbon atoms lying on the central symmetry axis (*b*).

If the number of magnetic nuclei is small and the hyperfine splitting exceeds the linewidth, one can resolve the hyperfine structure in the spectrum of triplet ODMR. For instance, the ODMR spectrum of a pentacene molecule deuterated at all positions except for two protons at the carbon atoms lying on the central symmetry axis exhibits a clearly seen hyperfine structure originating from two magnetically equivalent protons (a triplet with the 1 : 2 : 1 intensity ratio) and corresponding to the $T_x \rightarrow T_z$ (Fig. 3 *b*) transition with an electron – proton interaction constant of ~ 10 MHz (~ 3.6 Gs).[13]

At first glance, observation of hyperfine structure seems to be a mysterious phenomenon. In a single-molecule experiment, nuclear configurations (a total of four for two protons of the partially deuterated pentacene) should be fixed during the time taken for one excitation – fluorescence cycle ($S_0 \rightarrow T_z \rightarrow S_0$), which is of the order of $10^{-5} - 10^{-6}$ s. The unpaired electron of the triplet molecule must experience only one nuclear configuration. However, the spectral shape suggests that it somehow 'sees' all the four pairs of spin configurations, namely, $\alpha_n\alpha_n$, $\alpha_n\beta_n$, $\beta_n\alpha_n$ and $\beta_n\beta_n$ (here, α_n and β_n denote the proton spins; the pairs $\alpha_n\beta_n$ and $\beta_n\alpha_n$ are equivalent and correspond to identical nuclear configurations).

The answer to this enigma is simple. In single-molecule ODMR experiments, the molecule experiences over 10^6 cascade excitation – fluorescence cycles during the typical measuring time (usually, about 10 min). Hence, the number of 'arrivals' at the ground state with a residence time of 100 μs during each cascade cycle is the same. Due to the dipole interaction of pentacene protons with the nuclei of neighbouring molecules and other nuclei of the indicator pentacene molecule, this time appears to be sufficient for reorientation of the spins of the pentacene protons (in spectroscopy, this is called spin diffusion or spectral diffusion). As a result, the pentacene protons have time to 'arrive' at all the four nuclear configurations during the ODMR measuring time and the final spectrum exhibits a triplet with the 1 : 2 : 1 intensity ratio (see Fig. 3 *b*).

It should be noted that reorientation of the proton spins (spectral diffusion) occurs only at those instants when the molecule is in the ground state. In the triplet state, strong electron – nuclear magnetic interaction fixes the proton spins and 'excludes' them from spectral diffusion (or, as spectroscopists say, excludes these protons from the dipole – dipole nuclear reservoir).

The hyperfine structure of the ODMR spectrum of ^{13}C nuclei of a pentacene molecule isotopically substituted at different positions is due to the same reasons.[14] However, it should be noted that all the ODMR spectra of single triplet molecules observed so far were measured for only one case, *viz*., a pentacene molecule implanted in a terphenyl crystal. Further progress of this experimental technique and extension of the areas of its application is closely related to advances of optical detection of single molecules in crystals and on the surface of solids.[15]

Magnetic resonance of single spin carriers has been intensively developed. Recently, Köhler[16] has reported an excellent review concerning the state-of-the-art and prospects of studies in the field, so that there is no need to dwell on this point.

Mention may be made of one important circumstance: it is spectral diffusion and change in the nuclear spin configurations at a single electron spin that cause a remarkable phenomenon, *viz*., a single spin Hahn echo.[17] It should be remembered that spin echo (Hahn echo) appears as a result of coherent behaviour of a spin ensemble; the observation of a single spin Hahn echo confirms the ergodic theorem, according to which averaging over the ensemble is equivalent to averaging over time.

IV. Single-molecule tunnelling spectroscopy

Recently published series of pioneering studies on tunnelling vibrational spectroscopy[18–20] has promoted the transformation of scanning tunnelling microscopy from a 'topographic' method for monitoring the atom-molecular relief of a surface into a new powerful method of chemical physics, which allows one not only to 'see' a desired single molecule, but also to identify it from 'fingerprints' (the vibronic spectrum) and even follow its chemical fate. The last-mentioned circumstance seems to be of great value owing to the possibility of observation of chemical transformations of a single molecule, which has appeared for the first time. So far classical chemistry has been concerned with molecular ensembles even in the best versions of molecular beam techniques. Modern coherent chemistry also deals with single wave packets (ensembles of coherent molecules) rather than single molecules.[21]

Physically, the idea a single-molecule, resonance tunnelling vibrational spectroscopy[18] is very simple. If a scanning tunnelling microscope operates in the field emission mode and the tip voltage exceeds the work function of electrons, the tunnelling electrons leaving the tip appear to be confined in the space between the tip and the adsorbed molecule 'sitting' on the surface under the tip. The electrons confined in this space can move between two potential barriers, *viz*., the tip and the surface. The residence time of an electron under the tip is of the order of $10^{-13} - 10^{-14}$ s (it is much longer than the mean free time), *i.e*., the space between the tip and the surface represents a specific nanoscale resonator in which standing waves (field emission resonances) appear at particular energies. Since the resonance energy depends on the tip potential, the tunnelling current as function of the bias voltage exhibits some clearly seen peaks corresponding to vibronic (resonance) energy levels of the specified adsorbed molecule which interacts with an the electron trapped in the resonator. This is a specific form of manifestation of a fundamental quantum effect called resonance bleaching of double potential barriers. Such barriers can be as 'wide and high' as it is wished, but if the

energy of the species corresponds to that of a quasi-stationary level, they appear to be penetrable.[22] The double potential barriers for which the energy of the tunnelling species can vary [23] (*e.g.*, thin layers of a dielectric containing impurity atoms or the tunnelling contacts containing adsorbed molecules) also appear to be penetrable.

In such systems, energy exchange between the tunnelling electrons and vibrational degrees of freedom of the impurity atoms or adsorbed molecules can occur, thus leading to excitation of oscillations (inelastic interaction). For those electrons whose energies correspond to those of vibronic levels of the resonator containing an adsorbed molecule, the vacuum gap between the surface and the tip becomes transparent; in this case, the tunnelling current is a maximum.

V. Tunnelling spectroscopy of a single electron spin

Tunnelling spectroscopy also allows detection of a single electron spin on the surface. This requires that the tunnelling electron be able to distinguish (discriminate) two spin states of the unpaired electron with $S_z = \pm 1/2$ (*e.g.*, the Zeeman energy levels of a paramagnetic species). There are two parameters suitable for performing such a discrimination, *viz.*, energy and spin. In typical magnetic fields $H \approx 3000$ Gs, the Zeeman energy of the unpaired electron is $\sim 10^{-5}$ eV, which is 4–5 orders of magnitude lower than the energies of the tunnelling electron and 3 orders of magnitude lower than the resolution of tunnelling spectroscopy (~ 0.01 eV). Clearly, it is impossible to use energy as a parameter for discriminating the Zeeman energy levels of the unpaired electron. This means that the other parameter, spin, should be used and that the detection principles of a single spin should be based on the spin chemistry laws.

Let us consider from this viewpoint the spin states and spin dynamics of two electron spins, the spin of a paramagnetic (probed) centre and that of a tunnelling (probing) electron. This two-spin system represents a spin analogue of the radical pair considered in the spin chemistry. It can be in two states, *viz.*, in a singlet state with the total spin S = 0 or in the triplet state with the total spin S = 1.

The energy splitting between these spin states equals the exchange energy J of two electrons in the nanoscale resonator. This means that all vibronic levels of the spin carrier situated under the tip should be split into doublets corresponding to the singlet and triplet spin states of the electron pair. The nanoscale resonator is 'transparent' to the tunnelling electrons of the electron pair irrespective of the state (singlet or triplet) of the pair at different energies (different tip potentials).

The interaction between two electrons (the tunnelling electron and the unpaired one) is identical to the interaction between radicals in a radical pair. For instance, recombination of a singlet radical pair, CH_3 and OH, involves the singlet channel only to give a singlet CH_3OH molecule, while their disproportionation involves the triplet channel (the reaction $CH_3 + OH \rightarrow {}^3CH_2 + H_2O$) to give the triplet carbene ${}^3CH_2$. Thus, formally, both channels are spin-allowed (*i.e.*, the total spins of the reagents and products in each channel conserve). However, the energy 'cost' of each channel is different, *viz.*, the former process proceeds barrierlessly (without activation energy), whereas the latter requires the overcoming of an energy barrier of ~ 6 kcal mol^{-1}.

Tunnelling spectroscopy of a single electron spin on the surface was theoretically substantiated and experimentally implemented by Dalidchik and Kovalevskii.[24] The spectrum of a O_2^- anion sitting on the TiO_2 surface (Fig. 4) exhibits a doublet splitting of each line, which is in complete agreement with theory. The splittings *1–2*, *2–3*, *1′–2′* and *2′–3′* equal 0.15 eV, which exactly corresponds to the vibrational quantum for the O–O bond in the anion (the frequency of the stretching vibrations O–O is 1180 cm^{-1}). Singlet–triplet splitting between the peaks, *i.e.*, the separations between the lines *1–1′*, *2–2′* and *3–3′*, is equal to the exchange energy of two electrons (the tunnelling

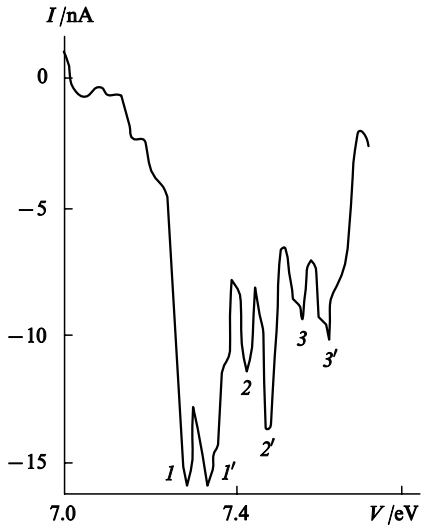


Figure 4. Tunnelling current I as function of the tip potential V (tunnelling spectrum) of a single radical anion O_2^- on the TiO_2 surface.

electron and the unpaired electron of the radical anion O_2^-) in the nanoscale resonator.

This experiment also allowed the exchange energy to be measured ($J = 0.07$ eV), which provided the possibility of estimating the size of the nanoscale resonator, R. Let us write the known relationship

$$J(R) = J_0 \exp(-\alpha R),$$

where J_0 is the exchange energy in a strongly coupled two-electron system (*e.g.*, H_2 molecule) and α is the characteristic parameter of the J decay as a function of R. Assuming that $J_0 \approx 4.5$ eV and $\alpha \approx 2$ Å^{-1}, we get $R \approx 2.1$ Å, which seems to be physically realistic for the nanoscale resonator.

VI. Tunneling spectroscopy of spin channels

As mentioned above, a single paramagnetic species can be detected using tunnelling spectroscopy due to the appearance of two resonance channels (a singlet and a triplet one) of the tunnelling current. These channels are separated by ~ 0.1 eV on the energy scale. Such a doublet splitting of vibronic levels was confirmed experimentally and discussed above (see Fig. 4). Equidistant doublet splitting of all lines in the tunnelling spectrum (on the plot of the dependence of the current I on the potential V) is an unambiguous indicator of the presence of a spin carrier (a radical or an ion) under the tip. However, direct attribution of each of the two spin channels to the singlet and triplet channel is impossible (we cannot determine to which channel the groups of lines *1*, *2* and *3* and *1′*, *2′* and *3′* in Fig. 4 belong). Based on general considerations and following Pauli, one can only suggest that the triplet level lies above the singlet one on the energy scale, *i.e.*, that the low-energy lines of the doublets correspond to the singlet channel, while their high-energy components correspond to the triplet channel. However, these considerations seem to be quite unreliable since no details of the interaction between the tunnelling electron and paramagnetic centre are currently known.

Microwave pumping is also unhelpful in distinguishing these channels since the singlet channel is ESR 'silent' while the response of the triplet channel (transitions between the states T_+, T_0 and T_-) does not produce any changes in the tunnelling current. Therefore, if microwave pumping causes no transitions between the states S and T, no transfer of the tunnelling electrons between the two channels occurs. On the other hand, yet another reason seems to be stronger: the lifetime of the electron pair in the nanoscale resonator is much shorter than the time taken for spin reorientation induced by microwave pumping. This means that

classical ESR of a single electron spin is impossible and other approaches should be used.

Imagine that the tip of a tunnelling microscope is made of a ferromagnetic material and emits spin-polarised electrons. (Such tips are widely used in topographic studies of the surface of ferromagnetic materials.[25]) If the voltage is chosen in such a way that the nanoscale resonator is 'tuned' in resonance with the singlet level, the potential barrier on the surface is transparent to the tunnelling electrons with the spins antiparallel to the spin of the paramagnetic centre. The singlet spin state of two electrons (the tunnelling electron and the unpaired one) in the nanoscale resonator is of course a combination of the spins of these electrons. Let the emitted (polarised) electrons leaving the paramagnetic tip have the spin β and the unpaired electron of the paramagnetic centre have either the spin α of β (here, the difference between the populations of the Zeeman energy levels of the electrons is neglected and the probabilities of the appearance of electrons with the spins α and β are taken to be equal). Then, the combinations αβ correspond to the singlet state of the electron pair, thus providing conditions for the tunnelling current to flow, while the combinations ββ correspond to the triplet state whose energy differs by a value of J. For the spin combinations ββ the potential barrier is impenetrable, so this contribution to the tunnelling current is locked.

Here, an important point which was first reported by Kozhushner *et al.*[26,27] should be taken into account. Due to exchange interaction between the electrons (more exactly, its nonsecular term $(1/2)J(S_+S_- + S_-S_+)$, where S_+ and S_- are the spin operators which increase and decrease the spin projection, respectively), the polarised electrons leaving the tip also polarise the spin of the unpaired electron in such a manner that its α spin it transformed into a β spin and the energy level α of the paramagnetic centre is depopulated. The system undergoes a transition from the singlet state to the triplet state and the resonance tunnelling current in the singlet channel no longer flows.

An energy level diagram illustrating the population of the Zeeman levels of both electrons in the system 'ferromagnetic tip – paramagnetic centre' is shown in Fig. 5. Initially (*a*), both energy levels corresponding to the single spin have nearly equal populations. If the tip potential differs from zero, the tunnelling current I_t proportional to $N_\beta P_\alpha$ (N_β is the population of the Zeeman energy level of the polarised tip electrons and P_α is the population of the upper Zeeman energy level α of the paramagnetic centre) flows in the system. The singlet current will flow only provided that the single spin of the paramagnetic centre will be oriented antiparallel to the spins of the tunnelling electrons, *i.e.*, in the combination βα.

It is known that

$$\frac{P_\alpha}{P_\beta} = \exp\left(-\frac{g\beta H}{kT}\right),$$

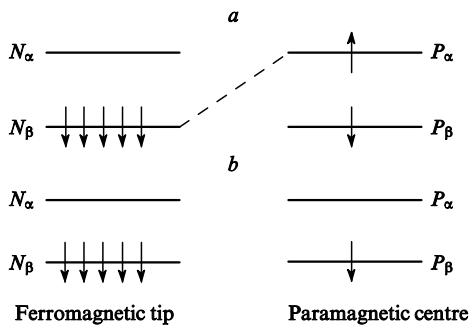


Figure 5. An energy level diagram illustrating population of the Zeeman levels in the system 'ferromagnetic tip – paramagnetic centre'. Initial state (*a*) and after passage of the tunnelling current (*b*).

where $g\beta H$ is the Zeeman splitting. Since $g\beta H \ll kT$, we get $P_\alpha \approx P_\beta$. Exchange interaction causes polarisation of the spin α of the paramagnetic centre (an analogue of the flip-flop transition in the nuclear Overhauser effect) and depopulation of the upper Zeeman energy level. As a result, only the spin combinations ββ remain in the system (Fig. 5*b*). The singlet resonance peak on the $I-V$ plot disappears and the tunnelling current (singlet channel) is locked.

The polarisation mechanism of the singlet tunnelling current lock has not been experimentally observed so far. However, should it be found, it could be possible to distinguish between the singlet and triplet channels of the resonance tunnelling current and to determine not only the magnitude, but also sign of the electron – electron exchange interaction in the nanoscale resonator. This opens new prospects for single-molecule tunnelling spectroscopy.

VII. Single electron spin relaxation

Observation of the lock effect of the singlet tunnelling channel requires that the spin of the paramagnetic species be completely polarised. This is possible only in the case of slow spin – lattice relaxation where the spin orientation of the species remains fixed between the acts of electron transport between the ferromagnetic tip and the surface. For characteristic spin relaxation times ($\tau_s \approx 10^{-8}$ s), this condition is met if the tunnelling currents are rather heavy, $I > 0.1$ nA s^{-1}. At weaker tunnelling currents, the species can have random spin orientations at the instances corresponding to the acts of interaction with the tunnelling electron; this means that both parallel and antiparallel orientations of the spins of the species and the electron are possible. During the measuring time of the tunnelling current (at specified voltage), the paramagnetic species sequentially interacts with numerous electrons leaving the tip (the number of electrons is $N = It$, where t is the measuring time). The probabilities of the singlet and triplet states of electron pairs are determined not only by the statistics of these states, but also by the kinetics of both spontaneous (relaxation) spin transitions and those induced by the polarised electron current.

In the case of ferromagnetic tip the lock rate of the singlet channel is given by the relation

$$\frac{\partial P}{\partial t} = -\left(I - \frac{1}{\tau_s}\right). \quad (1)$$

Here, P is the population of the singlet channel (*i.e.*, the population of the spin states αβ) and I is the tunnelling current of those electrons that had experienced exchange scattering by the paramagnetic centre. The first term in Eqn (1) includes the polarisation of the paramagnetic centre due to the polarised electron current (the pumping rate of the triplet channel and the depopulation rate of the singlet channel) while the second term includes the depolarisation (relaxation) rate of the triplet channel and the recovery rate of the singlet channel.

If $I > \tau_s^{-1}$ ($\partial P/\partial t < 0$), population of the triplet channel and depopulation of the singlet channel occur; the tunnelling current in the singlet channel is locked. At weak currents, where $I < \tau_s^{-1}$ ($\partial P/\partial t > 0$), the relaxation rate is higher than the population rate of the triplet channel. In this case, the weak tunnelling current cannot lock the singlet channel that remains open. In fact, the condition $I = \tau_s^{-1}$ determines the lock threshold of the tunnelling current. It allows measurements of the electron spin relaxation time of the single paramagnetic centre under conditions of tunnelling spectroscopy.

VIII. Can single-spin ESR be detected by tunnelling spectroscopy?

Novel spin spectroscopy methods, *viz.*, optical spectroscopy and tunnelling spectroscopy are based on spin combinations of two

electrons. In both cases, not only detection of single paramagnetic species, but also measurements of their spin relaxation parameters is possible. However, these methods use fundamentally different detection techniques. In the case of optical detection, the singlet channel manifests itself *via* fluorescence and, hence, some of its characteristics can be measured. The triplet channel is nondetectable; however, both the channels are strongly coupled *via* the spin–orbit and magnetic interactions, so that any changes in the triplet (nondetectable) channel affect some parameters of the singlet channel. In tunnelling spectroscopy, both these channels are detectable; however, no magnetic interaction between them occurs so that they are independent.

There is also a number of dynamic distinctions between the two above-mentioned detection techniques. In the case of optical detection, the residence time of a molecule in the triplet state is $\sim 10^{-5}$ s in each excitation–deactivation cycle. This time is much longer than that required for spin reorientation under the action of microwave pumping, $\tau_{mw} = (\gamma H)^{-1}$ (γ is the gyromagnetic ratio of an electron and H is the strength of the microwave field). Typically, $\tau_{mw} \approx 3.1 \times 10^{-7}$ s; this means that the triplet lifetime is long enough for both spin reorientation and change in the populations of the triplet levels under the action of the microwave magnetic field. In other words, the triplet state is an effective 'receiver' of external microwave radiation. In tunnelling spectroscopy, the residence time of the electron in the nanoscale resonator is very short. As mentioned above, it does not exceed 10^{-14} to 10^{-13} s. This means that the triplet states in the nanoscale resonator cannot act as effective 'receivers' of microwave radiation.

In tunnelling microscopy, single-spin magnetic resonance should be detected using non-classical approaches (*e.g.*, polarised tunnelling electrons).

In this case, the population kinetics of the spin states is similar to that considered above; however, transitions between two spin orientations of a paramagnetic species can now be stimulated not only by the tunnelling electrons, but also by microwave pumping.

This can be easily understood by considering Eqn (1) again. If resonance microwave pumping occurs (*i.e.*, the ESR conditions are met), this equation takes the form

$$\frac{\partial P}{\partial t} = -\left(I - \frac{1}{\tau_s} - \frac{1}{\tau_{mw}}\right). \qquad (2)$$

As can be seen, a new term appears, which is due to the spin relaxation induced by the microwave pumping. Spin relaxation induces additional transitions from the state ββ to the state αβ, thus additionally populating the singlet channel with a rate of τ_{mw}^{-1}. In other words, microwave pumping shifts the lock threshold of the singlet channel in such a manner that the old condition $I = \tau_{mw}^{-1}$ is replaced by a new one,

$$I = \frac{1}{\tau_s} + \frac{1}{\tau_{mw}}.$$

Since the values τ_s^{-1} and τ_{mw}^{-1} are commensurable under standard ESR conditions, the additional shift of the lock threshold of the tunnelling current in the singlet channel due to microwave pumping can be noticeable and even experimentally measurable. Moreover, experiments under conditions where $\tau_{mw}^{-1} \ll \tau_s$ can be readily set up (at $H \gg 1$ Œ). In this case, the shift of the lock threshold will be nearly completely determined by the microwave pumping. This offers considerable promise for single-spin ESR detectable from the tunnelling current. A complete theory of this phenomenon has been developed recently.[28]

IX. Excited states and single-molecule chemistry

In the aforesaid, we assumed conservation of the electron energy (it should be remembered that the Zeeman transition energies are negligible). Hence, the spin effects due to exchange interaction, relaxation and microwave pumping were associated solely with changes in the spin orientations of the paramagnetic species and tunnelling electrons. However, more complex effects can also occur, where the tunnelling electrons are responsible not only for the change in the spin orientation of the adsorbed species, but also for the excitation of internal (vibrational and/or electronic) degrees of freedom of the species. In the case of tunnelling between conductors in which all electron states below the Fermi level can be considered filled, such processes can proceed only at the voltages V exceeding the energy loss $\delta\varepsilon$ (usually, $\delta\varepsilon \gg tT$) and the dependence of I on the potential V exhibits the so-called threshold features (conductivity jumps), which appear at the voltage $eV = \delta\varepsilon$. Threshold features manifest themselves as maxima of the second derivatives of the tunnelling current with respect to the tip potential. They are observed in those cases where the tunnelling electrons excite the molecule 'sitting' under the microscope tip and induce its chemical transformations.

The possibility of observation of inelastic processes using tunnelling microscopy was predicted in 1985; however, experimental studies have been reported only recently.[29–31] For instance, it was found that molecules C_2H_2 and C_2D_2 adsorbed on the (001) surface of a copper single crystal dissociate to give C_2H and C_2D, respectively. This occurs at potentials of 2.8 V for C_2H_2 and 3.9 V for C_2D_2.[31] The C_2H and C_2D radicals thus formed undergo further dissociation to give C_2 at potentials of 2.1 and 2.7 V, respectively. In this case, large isotope effects are due to differences between the vibrational excitation cross-sections of different isotopomers rather than to isotopism of the C–H and C–D bonds. The excitation cross-section is determined by the probability of energy transfer (an inelastic process) from the 'light' tunnelling electron to the 'heavy' molecule; its magnitude is proportional to a small parameter $(a_0/R)^{2\Delta v} \leqslant 10^{-2\Delta v}$ (a_0 is the amplitude of zero-point vibrations of the molecule or constituent atoms, R is the characteristic atomic size and Δv is the change in the vibrational quantum number upon excitation). This formula readily demonstrates large isotope effect for the excitation cross-section.

Dehydrogenation was also observed for single ethylene molecules adsorbed on the Ni(110) surface (finally, ethylene loses two protons to give C_2H_2) and for benzene, pyridine and their isotopomers adsorbed on the Cu(001) surface.[31] Moreover, diffusion displacements and rotational motions of single molecules induced by the tunnelling electrons can also be observed along with their chemical transformations.

No observations of threshold features in the experiments on the excitation of adsorbed species by tunnelling electrons using a scanning tunnelling microscope (STM) have been reported so far. These features are assumed to be 'large-scale' since in this case we are concerned with electron–electron energy exchange. Of particular interest is consideration of a physically adsorbed oxygen molecule. The ground state of the molecule (a triplet $X^3\Sigma_g^-$) is separated from the nearest excited singlet state ($a^1\Delta_g$) by about 1 eV on the energy scale. The reactivity and relaxation of singlet dioxygen adsorbed on various surfaces were studied in detail by Ryskin [32] and Krylov and Shub.[33] Using different 'macroscopic', kinetic and spectroscopic methods, they first determined the relaxation times of singlet dioxygen. It was found that this parameter depends strongly on the surface characteristics and its magnitude can vary over a wide range. Optimum experimental conditions for observation of threshold features of the $X^3\Sigma_g \rightarrow a^1\Delta_g$ transitions of an oxygen molecule 'sitting' under the tip using a STM should be chosen so that the rates of stimulated and spontaneous (relaxation) transitions be comparable. This allows detection of new changes in the tunnelling current by varying the tunnelling current (*i.e.*, by changing the populations of two electronic states of the oxygen molecule). This situation is quite similar to that described above for the single spin ('self-regulation' and lock of the tunnelling current).

X. Single-molecule spin chemistry

In STM experiments, the operating current densities can be as high as 10^8 A cm^{-2}. It is for this reason that is possible to transform the equilibrium conditions into nonequilibrium ones and cause creation of nonequilibrium distributions over vibrational and electron energy levels of the single molecules 'sitting' under the tip.[34] (It should be remembered that in the case of single-molecule experiments we are dealing with ensembles of elementary events, *i.e.*, a manifold of independent interaction acts of a species with individual tunnelling electrons.) Heating leads to acceleration of chemical transformations such as desorption, dissociation, transfer of the adsorbed species from the tip to the surface, *etc*. Experiments with ferromagnetic tips allow the observation of versatile single-molecule spin chemistry effects. The simplest case is deposition of a paramagnetic species from the ferromagnetic tip on the surface containing a paramagnetic centre. It is easy to understand that at sufficiently heavy tunnelling currents (both species are polarised) recombination is forbidden. At weak currents (the spin of the species adsorbed on the surface has no definite orientation), recombination is allowed.

XI. Conclusion

Thus, classical scanning tunnelling microscopy gave impetus to the emergence and development of two new, important and promising methods, *viz*., single-molecule tunnelling spectroscopy and single-molecule chemistry.

The emergence of these methods signifies a new stage of the development of modern chemistry, which offers considerable prospects for surface sciences, catalysis, *etc*. In particular, the use of single-molecule spectroscopy and single-molecule chemistry in combination with photochemistry and femtochemistry presents new, inestimable possibilities for manipulating the molecules. In the framework of single-molecule spectroscopy and single-molecule chemistry classical spin chemistry also undergoes transformation into 'single-molecule' spin chemistry. This offers unique possibilities for spin channel detection, single electron spin manipulation and detection of ESR of a single paramagnetic centre (including triplet molecules, carbenes and ions) from the tunnelling current.

The authors express their gratitude to the Russian Foundation for Basic Research and the Federal Programme 'Integration' for financial support.

References

1. D Attanasio *EPR Newsletters* **9** 14 (1998)
2. D Attanasio, D Capitani, C Federici, A Serge *Archaeometry* **37** 377 (1995)
3. A G Semenov, N N Bubnov *Pribory Tekhnika Eksperim*. (1) 92 (1959); *Vestn. Akad. Nauk SSSR* (3) 55 (1959) [a]
4. O Ya Grinberg, A A Dubinskii, Ya S Lebedev *Usp. Khim*. **52** 1490 (1983) [*Russ. Chem. Rev*. **52** 850 (1983)]
5. E L Frankevich, A I Pristupa, V I Lesin *Chem. Phys. Lett*. **47** 304 (1978)
6. A L Buchachenko, E L Frankevich *Chemical Generation and Reception of Radio- and Microwaves* (New York: VCH, 1994)
7. V O Saik, O A Anisimov, Yu N Molin *Chem. Phys. Lett*. **116** 138 (1985)
8. O A Anisimov, V M Grigoryants, Yu N Molin *Pis'ma Zh. Eksp. Teor. Fiz*. **30** 589 (1979)
9. S Mais, J Tittel, Th Basché, C Bräuchle, W Göhde, H Fuchs, G Müllen, K Müller *J. Phys. Chem. A* **101** 8435 (1997)
10. W E Moerner, M Orrit *Science* **283** 1670 (1999)
11. F Kulzer, F Koberling, Th Crist, A Mews, Th Basché *Chem. Phys*. **247** 23 (1999)
12. J Köhler, J A J M Disselhorst, M C J M Donckers, E J J Groenen, J Schmidt, W E Moerner *Nature (London)* **363** 242 (1993)
13. J Wrachtrup, C von Borczyskowski, J Bernard, M Orrit, R Brown *Nature (London)* **363** 244 (1993)
14. J Köhler, A C J Brouwer, E J J Groenen, J Schmidt *Science* **268** 1457 (1995)
15. *Chem. Phys*. **247** (1) (Spec. Issue) (1999)
16. J Köhler *Phys. Rep*. **310** 261 (1999)
17. J Wrachtrup, C von Borczyskowski, J Bernard, R Brown, M Orrit *Chem. Phys. Lett*. **245** 262 (1995)
18. F I Dalidchik, M V Grishin, N N Kolchenko, S A Kovalevskii *Surf. Sci*. **387** 50 (1997)
19. F I Dalidchik, M V Grishin, S A Kovalevskii, N N Kolchenko *Pis'ma Zh. Eksp. Teor. Fiz*. **65** 306 (1997)
20. S A Kovalevskii, F I Dalidchik, M V Grishin, N N Kolchenko, B R Shub *Appl. Phys. A, Mater. Sci. Process*. **66** (Suppl. Pt. 1) (1998)
21. A L Buchachenko *Usp. Khim*. **68** 99 (1999) [*Russ. Chem. Rev*. **68** 85 (1999)]
22. D Bohm *Quantum Mechanics* (New York: Prentise Hall Inc., 1952)
23. F I Dalidchik *Zh. Eksp. Teor. Fiz*. **87** 1384 (1984)
24. F I Dalidchik, S A Kovalevskii *Pis'ma Zh. Eksp. Teor. Fiz*. **67** 916 (1998)
25. R Wiesendanger, in *Scanning Probe Microscopy. Analytical Methods* (Berlin: Springer, 1998)
26. M A Kozhushner, B R Shub, R R Muryasov *Pis'ma Zh. Eksp. Teor. Fiz*. **67** 484 (1998)
27. A L Buchachenko, M A Kozhushner, B R Shub *Izv. Akad. Nauk, Ser. Khim*. 1732 (1998) [b]
28. A L Buchachenko, F I Dalidchik, B R Shub *Chem. Phys. Lett*. **340** 103 (2001)
29. B C Stipe, M A Resaei, W Ho *Phys. Rev. Lett*. **81** 1263 (1998)
30. B C Stipe, M A Resaei, W Ho *Science* **279** 1907 (1998)
31. J Gaudioso, H J Lee, W Ho *J. Am. Chem. Soc*. **121** 8479 (1999)
32. M E Ryskin, Candidate Thesis in Physicomathematical Sciences, Institute of Chemical Physics, Academy of Sciences of the USSR, Moscow, 1983
33. O V Krylov, B R Shub *Neravnovesnye Protsessy v Katalize* (Non-Equilibrium Processes in Catalysis) (Moscow: Khimiya, 1990)
34. M V Grishin, F I Dalidchik, S A Kovalevskii, N N Kolchenko *Pis'ma Zh. Eksp. Teor. Fiz*. **71** 104 (2000)

[a] — *Herald Russ. Acad. Sci. (Engl. Transl.)*
[b] — *Russ. Chem. Bull. (Engl. Transl.)*